ERJ Express. Published on February 25, 2010 as doi: 10.1183/09031936.00065809

Characterization of cell adhesion in airway epithelial cell types using ECIS

Irene H. Heijink[1,2], Simone M. Brandenburg[1], Jacobien A. Noordhoek[1], Dirkje S. Postma[2], Dirk-Jan Slebos[2], Antoon J.M. van Oosterhout[1]

[1]Lab Allergology & Pulmonary Diseases, Department of Pathology & Medical Biology and [2]Department of Pulmonology, University Medical Center Groningen, University of Groningen, The Netherlands,

Corresponding author: Dr. I.H. Heijink, Laboratory Allergology & Pulmonary Diseases, Department of Pathology & Medical Biology, University Medical Center Groningen, University of Groningen, Hanzeplein 1, NL-9713 GZ, Groningen, The Netherlands

Phone No: +31 (0)50 3610998

Fax No: +31 (0)50 3610570

E-mail: h.i.heijink@int.umcg.nl

[*]This study was supported by grant no. 3.2.05.039 from the Netherlands Asthma Foundation (NAF) and by GlaxoSmithKline

Running title: characterization of airway epithelial cells by ECIS

Abstract

Research on epithelial cell lines and primary epithelium is required to dissect the mechanisms underlying structural abnormalities in airway epithelium as observed for respiratory diseases, including asthma and COPD.

We used the novel technique Electric Cell-Substrate Impedance Sensing (ECIS) to monitor cell adhesion/spreading, barrier function and wound healing. We compared primary bronchial epithelium with airway epithelial cell lines 16HBE14o-, BEAS-2B, NCI-H292 and A549.

We demonstrate that BEAS-2B, A549 and primary cells form a confluent monolayer more rapidly than 16HBE14o- cells. In contrast, 16HBE14o- cells form stronger intercellular contacts, with a 10-fold higher resistance than BEAS-2B, A549 and NCI-H292 cells and a 5-fold increase over primary cells. Accordingly, expression of the adhesion molecules ZO-1 and E-cadherin was highest in 16HBE14o-. These molecules were localized in intercellular junctions in both 16HBE14o- and primary cells. Finally, restoration of barrier function upon injury was impaired in BEAS-2B when compared to 16HBE14o-.

In conclusion, epithelial cell types display remarkable phenotypic differences and should accordingly be used to address specific research questions. 16HBE14o- cells appear most suitable for studies on barrier formation, while resemblance in attachment of primary cells to BEAS-2B and A549 cells makes the latter more important for translational research on cell-matrix contact.

Key words: adhesion molecules, airway epithelial injury, epithelial repair, respiratory disease, tight junctions.

Abbreviations: adherens junctions, AJs; air-liquid interface, ALI; Electric Cell-Substrate Impedance Sensing, ECIS; extracellular matrix, ECM; filamentous actin, F-actin; primary bronchial epithelial cells, PBEC; transepithelial resistance, TER; tight junctions, TJs; zona occludens, ZO-1.

Introduction

The airway epithelium plays a central role in the pathogenesis of various pulmonary diseases, including asthma, COPD and cystic fibrosis. In healthy subjects, the respiratory epithelium acts as a physical barrier to harmful inhaled substances, e.g. allergens, cigarette smoke and pathogens. Epithelial barrier function is maintained by intercellular contact formation in so-called adherens junctions (AJs) and tight junctions (TJs). AJs regulate adhesion through homotypic interactions of the adhesion molecule E-cadherin on adjacent cells, providing the architecture required for TJs (1). TJs are localized more apically, comprise the interacting proteins occludin, claudins and zona occludens (ZO)-1 and restrict paracellular permeability. Under pathological conditions, disruption of epithelial integrity and/or inefficient epithelial repair may lead to increased access of environmental factors, e.g. allergens, to subepithelial layers. Indeed, the airway epithelium is often damaged in asthma, with increased permeability and loss of E-cadherin and ZO-1 expression (2-4). Disruption of the epithelial barrier may also relate to structural abnormalities and epithelial remodelling, i.e. mucous hyperplasia and squamous cell metaplasia, as observed in COPD (5;6).

Rapid restoration of the epithelial barrier upon injury is crucial and may be distorted in patients suffering from respiratory diseases like asthma and COPD. Complete regeneration of the airway epithelium requires epithelial migration, proliferation and reconstitution into a well-differentiated epithelium that forms functional intercellular junctions. Better characterization of cell adhesion during growth and repair processes is thus pivotal to the search for new therapeutic strategies. Moreover, it is of importance to use a cell line with high translational value

for the *in vivo* situation. Since different cell lines vary in their capacity to form cell-cell contacts (7), we compared adhesive abilities of the bronchial epithelial cell lines 16HBE14o- and BEAS-2B, the mucoepidermoid carcinoma cell line NCI-H292, the alveolar type-II carcinoma cell line A549 and primary bronchial epithelial cells (PBEC). We measured epithelial resistance using ECIS, a novel technique that enables accurate, real time monitoring of epithelial resistance, with the ability to distinguish between different processes that contribute to changes herein, i.e. cell attachment and formation of intercellular junctions (8). Additionally, we used the ECIS system to reproducibly and quantitatively study differences in epithelial repair and barrier recovery upon wounding by electroporation. Finally, we studied whether differences between airway epithelial cells types relate to differences in the expression of cell-cell contact molecules.

Methods

Cell culture

The human bronchial epithelial cell line 16HBE14o- was kindly provided by Dr. D.C. Gruenert (University of California, San Francisco, CA) and cultured in EMEM medium/10% FCS (Biowhittaker, Verviers, Belgium) on collagen-coated flasks as described (9). Human bronchial BEAS-2B cells were cultured in RPMI medium/10% FCS on collagen-coated flasks. The carcinoma cell lines NCI-H292 and A549 were cultured on uncoated flasks in RPMI medium/10% FCS. All culture media were supplemented with 100 U/ml penicillin and 100 μg/ml streptomycin. PBEC from bronchial brushings in asthma, COPD and healthy control subjects were obtained and cultured as described previously (10-12). Cells were cultured in hormonally supplemented bronchial epithelium growth medium (BEGM, Lonza, Walkersville, MD), in flasks coated with collagen and fibronectin (13) and used for experiments at passage 2. Epithelial cells from healthy donors were used for both ECIS and immunodetection/staining *(n=3)*. Epithelial cells derived from COPD and asthma patients were used for either immunodetection/staining (*n=3*) or ECIS (*n=1*).

ECIS

The resistance of cells in culture was measured using ECIS as described previously (8). All tested cell lines were grown on collagen-coated arrays, whereas primary cells were grown on fibronectin plus collagen-coated arrays. Cell adhesion measurements were based on changes in resistance/capacitance to current flow applied to the electrode arrays at different frequencies (Applied Biophysics, Troy, NY). A frequency scan was performed to test for the frequency at which the largest difference in values of epithelial resistance was obtained between the cell-covered and cell-free electrodes.

The baseline was established with culture medium (400 µl/well) alone and compared to the electrodes covered with a monolayer of cells in 400 µl medium. The optimal frequency to study resistance appeared to be 400 Hz. For the resistance/capacitance measurements, cells were inoculated at $75*10^3$cells/well or other when indicated in 400 µl in duplicate. Wounding was performed by electroporation using voltage pulses of 5V and 40 kHz, for 30 sec.

Air liquid interface

For air–liquid interface (ALI) cultures, cells were grown to confluence, harvested and seeded at $50*10^3$cells/insert on semi-permeable membranes (Trans-well, 0.4 µm pore-size, 12 mm diameter, Corning Incorporated; Cambridge, MA) coated with 30 µg/ml collagen and 10 µg/ml BSA. Cells were cultured in a 1:1 mixture of DMEM (Lonza) and BEGM supplemented with retinoic acid (RA, 15 ng/ml; Sigma) and grown submerged until confluence (4–7 days) after which they were exposed to an air–liquid interface for another 2-4 weeks. Mucociliary differentiation was observed between day 14 and 26 after exposure to air–liquid interface. Transepithelial resistance (TER) was measured using a voltohmmeter (EVOM, World Precision Instruments, Sarasota, FL), which differs from ECIS in surface area (1.12 cm^2 for the porous membrane insert versus $0.5*10^{-3}$ cm^2 for the electrodes in the ECIS system), applied current (20 µA versus 1 µA in the ECIS system) and the inability to measure at different frequencies and thereby distinguish between cell-cell and cell-matrix contacts.

siRNA downregulation of E-cadherin

E-cadherin gene expression was downregulated in the 16HBE14o- cells by the use of siRNA as described before (9). In short, cells were seeded at $5*10^4$cells/well and

transfected with E-cadherin-targeted siRNA/non-targeting control oligonucleotides (Eurogentec, Liege, Belgium) in a final concentration of 20 μM using Oligofectamine (Invitrogen corporation, Carlsbad, CA).

Immunodetection by western blotting

Total cell lysates were obtained by resuspension of the cells in Laemmli buffer and immunodetection was performed as described (9), using anti-E-cadherin (Santa Cruz Biotechnology, Santa Cruz, CA) and anti-ZO-1 (Zymed, San Francisco, CA).

Immunofluorescent staining

Cells grown on LabTeks were washed with PBS/$CaCl_2$, fixed in ice-cold acetone (90%) for 30 min, blocked in PBS/5% BSA for 60 min, incubated for 60 min with primary antibodies (1:200) and subsequently incubated for 60 min with FITC-labeled anti-rabbit (1:200, DAKO Diagnostics, Mississauga, ON, Canada) or Rhodamine-labeled anti-mouse IgG conjugates (1:400, Jackson Immunoresearch Laboratories, West Grove, PA) or rhodamine-labeled phalloidin (1:200, Cytoskeleton Inc, Denver, CO) in presence of DAPI (1:500) and analyzed as described (14).

Results

Characteristics of 16HBE14o- attachment and cell-cell contact formation

We first tested human bronchial epithelial cells 16HBE14o- by monitoring the capacitance of the monolayer at a high frequency (40 kHz) and the resistance at a low frequency (400 Hz). The epithelial resistance and the current flow in the adhesion area of the cells are dependent on the frequency of the applied current. Wegener *et al* (8) have shown that, when monitoring growth and attachment, resistance is most sensitively measured at a low frequency (low-frequency resistance). At low frequencies (200-5000 Hz), the resistance increased during the initial attachment and spreading phase, going through a period of slow increase and then rising to the final levels, which is thought to be due to the establishment of tight junctions. The capacitance measurements, on the other hand, appeared relatively insensitive to changes at low frequencies, getting more sensitive to changes due to cell attachment/spreading when moving to higher frequencies. In contrast to the resistance, the capacitance measurements were barely affected by the formation of intercellular junctions. These data suggest that changes in high-frequency capacitance are most likely caused by cell attachment, spreading and growth and that the low-frequency changes, when not paralleled by changes in high-frequency capacitance, are most likely the consequence of intercellular junction formation.

Cells inoculated at a concentration of $75\text{-}100*10^3$ reached confluence between 30-50 hours, as established by an initial decrease followed by stabilization of the high-frequency capacitance (Fig. 1B), which is inversely related to resistance. During the initial spreading/attachment of the cells within the first 40 hours, only a minimal increment could be observed in the low-frequency resistance (Fig. 1A) and the

marked increase upon stabilization of the capacitance at 40-60 to 80 hours most likely reflects the establishment of intercellular contacts. To confirm that the increase in low-frequency resistance during this period is a reflection of the formation of intercellular junctions, we studied the localization of the junctional proteins ZO-1 and E-cadherin upon inoculation. As expected, we observed a continuous circumferential localization of both ZO-1 and E-cadherin after 72 hours, while junctional expression of these proteins was still fragmented after 24 hours (Fig. 1C).

At a concentration of 25-50*10^3 cells/well, confluence was reached at 60-80 hours as confirmed by visual microscopic analysis (not shown); nevertheless, the cells were not able to form tight intercellular junctions efficiently within the time frame of our experiment, as demonstrated by the low-frequency resistance (Fig. 1A). Therefore, the inoculation of 75*10^3 cells was used further for all experiments described in this manuscript.

E-cadherin-mediated cell-cell contact formation is an important determinant in low-frequency resistance

To confirm the involvement of intercellular junctions in the increase in low-frequency resistance of 16HBE14o- cells, we monitored the changes upon siRNA downregulation of E-cadherin. We also measured the capacitance at a high frequency (40 kHz), which should be relatively insensitive to changes in cell-cell contacts. E-cadherin expression was already effectively downregulated at day 1 after transfection and remained downregulated during the course of the experiment (at least 72 hours, Fig. 2C). Low-frequency resistance increased from 24 to 60 hours in the control cells (Fig. 2A). Cells transfected with E-cadherin-targeted siRNA showed a far less pronounced increase (Fig. 2A). High-frequency capacitance measurements, on the

contrary, were not affected by the downregulation of E-cadherin (Fig. 2B), indicating that loss of E-cadherin-mediated junctions specifically affects low-frequency resistance measurements. TJ sealing has been reported as major determinant in electrical resistance (15), while prior formation of AJ may be required for proper assembly of TJs (16). We therefore analyzed expression of the TJ protein ZO-1 and observed reduced levels upon siRNA downregulation of E-cadherin (Fig. 2D).

To find further support for the sensitivity of low-frequency resistance to the formation of intercellular junctions, we depleted the 16HBE14o-monolayer of Ca^{2+}, given the fact that epithelial junctions are completely Ca^{2+} dependent. Ca^{2+} deprival resulted in a dramatic decrease in low-frequency resistance towards the levels of uncovered electrodes (Fig. 2E). In accordance, immunofluorescent staining revealed a complete loss of junctional expression of E-cadherin (Fig. 2F).

Comparison of 16HBE14o-, BEAS-2B, H292 and PBEC

We were interested to study the specific adhesive characteristics of different human airway epithelial cells and observed marked differences. BEAS-2B cells were relatively inefficient in the formation of intercellular junctions when compared to 16HBE14o- cells, as reflected by a 10-fold lower resistance (Fig. 3A). In contrast, BEAS-2B cells established a confluent monolayer more rapidly, with a strong decline in capacitance within 3 hours upon inoculation (Fig. 3A). After stabilization of the capacitance values, the low-frequency resistance only marginally increased to a maximum of approximately a 2.5-fold increase, in contrast to the strong increase in barrier tightness of the 16HBE14o- cells. A549 cells showed similar characteristics to BEAS-2B cells, with a rapid formation of a confluent layer. After this, low-frequency resistance did not further increase, suggesting that the initial increase was merely due

to coverage of the electrodes without formation of tight junctions (Fig. 3B). NCI-H292 cells were also inefficient in establishing intercellular junctions (Fig. 3C), with a slow and weak increase in low-frequency resistance over time that followed the kinetics of high-frequency capacitance.

Of all tested cells types, PBEC showed the most rapid initial decrease in capacitance, reaching its minimum within 2 hours (Fig. 3D). Remarkably, this was followed by a temporary increase before values started to decline again (Fig. 3D). These dynamics appear to be a specific hallmark of PBEC and might be caused by alterations in cell shape, with initial attachment/spreading followed by adaption of a less flattened cell shape, e.g. to prepare for proliferation. During the first 48 hours, the primary cells showed only a modest increase in low-frequency resistance, with a similar fluctuation as observed for the high-frequency capacitance. The resistance markedly increased upon 55-60 hrs (after cells were hormone/growth factor-deprived), resulting in a 4-7 fold increase over the initial values (versus a 25-fold increase in 16HBE14o-). Finally, we measured transepithelial resistance (TER) of PBECs grown at the air-liquid interface (ALI), since PBECs can differentiate into a polarized mucociliary epithelium under these conditions (17), forming a tight epithelial barrier. It is not possible to measure the resistance of cells grown on trans-well membranes using ECIS. Therefore, we used a conventional voltohmmeter. Epithelial resistance markedly increased in PBEC grown under ALI conditions, from 151-190 $\Omega*cm^2$ at confluence under submerged conditions to levels up to 560-784 $\Omega*cm^2$ upon mucociliary differentiation. 16HBE14o- cells, on the other hand, established levels as high as 672-1120 $\Omega*cm^2$ (versus 60-100 $\Omega*cm^2$ measured on the ECIS electrodes) when grown under submerged conditions (EMEM/10%FCS), but

did not further increase their barrier tightness nor differentiated into mucociliary cells under ALI conditions (data not shown)

In conclusion, whereas PBECs adhere faster than 16HBE14o- cells and resemble A549 and BEAS-2B cells more closely in this respect, barrier tightness of PBECs is more comparable to 16HBE14o- cells, but their barrier will only become as tight as in 16HBE14o- cells when PBECs are grown under ALI conditions.

The ability to form epithelial junctions is related to the expression and localization of cell adhesion molecules

We next tested whether differences in barrier function of the individual monolayers were paralleled by expression of junctional proteins. In agreement with their barrier tightness, the ability of 16HBE14o- cells to form intercellular junctions was confirmed by the highest expression of ZO-1 (Fig. 4A), while reduced levels of ZO-1 were observed in A549, NCI-H292 and PBECs (healthy donor), and the lowest levels were expressed by BEAS-2B cells (Fig. 4A). E-cadherin was highly expressed in 16HBE14o-, NCI-H292 and primary cells, despite the lower capacity of NCI-H292 to form intercellular junctions. BEAS-2B and A549 cells expressed low levels of E-cadherin (Fig. 4A).

To validate whether the ECIS system can be a useful tool for the comparison of adhesive characteristics of epithelial cell lines, we studied epithelial cells derived from different individuals. Similar levels of E-cadherin were observed in PBEC from asthma, COPD and healthy subjects. In contrast, the expression of ZO-1 was markedly reduced in asthma epithelium (Fig. 4A, representative of 3 independent experiments). In accordance, we observed that low-frequency resistance was lowest in epithelial cells derived from an asthma patient when compared to healthy and COPD

cultures (isolated observation, Fig. 4B). Although we cannot draw any conclusions on the epithelial barrier function of asthmatics from this experiment, these data indicate that the ECIS is a promising tool to quantify differences in epithelial barrier tightness between different patient groups.

Since NCI-H292 cells expressed relatively high levels of ZO-1, despite the low barrier function, we also studied localization of ZO-1 and E-cadherin. Continuous circumferential localization of ZO-1 and E-cadherin in intercellular junctions is characteristic of cells that form occluding junctions. As expected, this was observed for 16HBE14o- cells (Fig. 4C). In contrast, expression of ZO-1 and E-cadherin was fragmented and discontinuous in NCI-H292 cells, offering an explanation for the impaired ability to form a tight barrier (Fig. 4C). In BEAS-2B, E-cadherin was hardly detectable by immunostaining, although a faint intercellular expression of ZO-1 could be observed (Fig. 4C). This may account for the increased barrier tightness of BEAS-2B versus NCI-H292 monolayers. The localization of E-cadherin and ZO-1 in the A549 cells resembled the expression pattern of NCI-H292 cells (Fig. 4C). In PBEC, intercellular junctions were present, as judged by the well-defined continuous expression of both ZO-1 and E-cadherin, although membrane expression of E-cadherin was less intensive than in the 16HBE14o- cells, and ZO-1 did not appear to separate each adjacent cell (Fig. 4C).

Dynamics in cytoskeletal actin filaments are thought to be the driving force of cell extension, flattening and attachment on the extracellular matrix (ECM) (18).We observed marked differences in cytoskeletal organization of filamentous actin (F-actin) between BEAS-2B, A549 and primary cells versus 16HBE14o- and NCI-H292 cells. F-actin was assembled in a stress fiber-like pattern in PBEC, A549 and BEAS-2B cells, whereas it was mainly localized parallel to the membrane in 16HBE14o- and

NCI-H292 cells (Fig. 4D). These differences may be linked to the differential kinetics of cell spreading and attachment as measured by high-frequency capacitance.

In conclusion, the extent and contiguity of E-cadherin, F-actin and particularly ZO-1 expression at intercellular junctions appears to correlate with adhesive characteristics of the cells. Table I presents an overview of the adhesive characteristics of the cell lines.

Migration and recovery of epithelial barrier upon wounding

In order to characterize the cell migration and regeneration response in the BEAS-2B and 16HBE14o- cells (which differed strongly in their cell-adhesive characteristics), we applied electric field-induced cell death and monitored subsequent morphological wound healing response. Using the ECIS system, the extent of the highly reproducible wound is restricted to the small 250-µm-diameter electrode, resulting in an almost complete detachment of the cells from the electrode (19), as confirmed by microscopy after washing away of the dead cells (Fig. 5A). This was accompanied by a dramatic drop in epithelial resistance and a corresponding increase in capacitance values (Fig. 5B). Within a couple of hours, cells started to spread and migrate over the electrode again (Fig. 5A), resulting in a decrease in capacitance and an increase in resistance (Fig. 5B). Complete coverage of the electrode by the 16HBE14o- cells was reached within 2 hours, as measured by high-frequency capacitance. From the time that a confluent monolayer was re-established, low-frequency resistance continued to increase slowly towards its original values, indicating reconstitution of intercellular junctions (Fig. 5B). In contrast, BEAS-2B cells showed no further increase in low-frequency resistance once the capacitance levels stabilized, which took approximately 2 hours longer than for 16HBE14o- (Fig. 5C). This indicates that the increase in

epithelial resistance is merely due to repopulation of the electrode and that BEAS-2B cells are unable to restore their tight junctions upon this type of injury. Thus, differences in cell-adhesive characteristics of BEAS-2B and 16HBE14o- are reflected by their wound healing response.

Discussion

This study shows that the ECIS system is a versatile tool to monitor various aspects of cell adhesion in airway epithelial cells during growth and repair. Measurement of epithelial resistance is a useful substitute for permeability assays, with possible difficulties due to diffusion of the solute. Furthermore, a major advantage of ECIS is that non-invasive real-time measurements can be performed at different frequencies. We demonstrate here that the high-frequency capacitance changes predominantly during initial cell spreading and attachment, but is hardly sensitive to alterations in intercellular junctions. The latter is most sensitively measured by resistance at a low frequency, enabling the distinction between intercellular and cell-matrix contacts.

We show large differences in adhesive characteristics between different airway epithelial cells, which can be related to the expression and/or localization of ZO-1 and E-cadherin (see Table I). Although A549, BEAS-2B and primary cells showed faster spreading/attachment, the highest barrier tightness was constituted by 16HBE14o- cells once confluence was reached. PBEC displayed moderate formation of TJs and AJs, as reflected by the junctional expression of ZO-1 and E-cadherin. Our findings further suggest that ZO-1 is a more important determinant in the formation of a tight epithelial barrier than E-cadherin. Our isolated observation on the lower formation of an epithelial barrier in asthma versus healthy epithelium is in agreement with the reduced expression of ZO-1, as also observed by others (2;3). We will further study barrier function of asthma patients in future studies.

The more rapid attachment of BEAS-2B, A549 and primary cells versus 16HBE14o- and NCI-H292 cells may result from differences in the dynamics of actin filament organization, which is thought to contribute to cell spreading/attachment

responses (18). Indeed, whereas F-actin showed a cortical localization in 16HBE14o- and NCI-H292, we observed stress fibers in PBEC and BEAS-2B cells. In addition to its function in attachment, the F-actin cytoskeleton is thought to regulate cell motility (20). The migratory response to injury appeared slower in BEAS-2B than in 16HBE14o- cells, suggesting that the observed F-actin arrangement in BEAS-2B cells favours cells attachment rather than cell motility.

Using the ECIS for wounding, cells need only migration, but not proliferation, to repopulate the electrode, since the electrodes are relatively small. This allows not only for more relevant but also more precise studying of the migration response compared to the scratch-wound method, where both proliferation and migration will take place during the 24 hours required to close the relatively large wound. *In vivo*, interaction with and remodelling of the ECM play a central role in epithelial cell migration, proliferation and restoration of the barrier during wound repair. This should be kept in mind for the translation to the *in vivo* situation. Still, complete regeneration of the airway epithelium requires reconstitution of intercellular contacts. Here we demonstrate that this is well reflected by ECIS measurements, as regeneration of the 16HBE14o- monolayer involved both migration and reconstitution of the barrier. In contrast, and as expected by their low-frequency resistance, BEAS-2B cells were inefficient to re-establish cell-cell contacts upon wounding.

In summary, we provide suggestive evidence for differential use of epithelial cell types in research on airway epithelial barrier function. The use of BEAS-2B and A549 cells may have high translational value in studies on cell attachment mechanisms. However, the functional TJ deficits of the BEAS-2B, A549 and NCI-H292 cell lines preclude their use in studies on epithelial barrier formation. 16HBE14o- may serve as a suitable model to study the behaviour of the bronchial epithelium with respect to

barrier function, cell-cell contact formation, permeability, epithelial-to-mesenchymal transition and the reconstitution of intercellular junctions upon wounding.

Reference List

(1) Gumbiner B, Stevenson B, Grimaldi A. The role of the cell adhesion molecule uvomorulin in the formation and maintenance of the epithelial junctional complex. J Cell Biol 1988 Oct;107(4):1575-87.

(2) de Boer WI, Sharma HS, Baelemans SM, Hoogsteden HC, Lambrecht BN, Braunstahl GJ. Altered expression of epithelial junctional proteins in atopic asthma: possible role in inflammation. Can J Physiol Pharmacol 2008 Mar;86(3):105-12.

(3) Holgate ST. The airway epithelium is central to the pathogenesis of asthma. Allergol Int 2008 Mar;57(1):1-10.

(4) Trautmann A, Kruger K, Akdis M, Muller-Wening D, Akkaya A, Brocker EB, et al. Apoptosis and loss of adhesion of bronchial epithelial cells in asthma. Int Arch Allergy Immunol 2005 Oct;138(2):142-50.

(5) Lapperre TS, Sont JK, van SA, Gosman MM, Postma DS, Bajema IM, et al. Smoking cessation and bronchial epithelial remodelling in COPD: a cross-sectional study. Respir Res 2007 Nov 26;8:85.:85.

(6) Kato Y, Hirano T, Yoshida K, Yashima K, Akimoto S, Tsuji K, et al. Frequent loss of E-cadherin and/or catenins in intrabronchial lesions during carcinogenesis of the bronchial epithelium. Lung Cancer 2005 Jun;48(3):323-30.

(7) Winton HL, Wan H, Cannell MB, Gruenert DC, Thompson PJ, Garrod DR, et al. Cell lines of pulmonary and non-pulmonary origin as tools to study the effects of house dust mite proteinases on the regulation of epithelial permeability. Clin Exp Allergy 1998 Oct;28(10):1273-85.

(8) Wegener J, Keese CR, Giaever I. Electric cell-substrate impedance sensing (ECIS) as a noninvasive means to monitor the kinetics of cell spreading to artificial surfaces. Exp Cell Res 2000 Aug 25;259(1):158-66.

(9) Heijink IH, Kies PM, Kauffman HF, Postma DS, van Oosterhout AJ, Vellenga E. Down-regulation of E-cadherin in human bronchial epithelial cells leads to epidermal growth factor receptor-dependent Th2 cell-promoting activity. J Immunol 2007 Jun 15;178(12):7678-85.

(10) Borger P, Kauffman HF, Scholma J, Timmerman JA, Koeter GH. Human allogeneic CD2+ lymphocytes activate airway-derived epithelial cells to produce interleukin-6 and interleukin-8. Possible role for the epithelium in chronic allograft rejection. J Heart Lung Transplant 2002 May;21(5):567-75.

(11) Heijink IH, Postma DS, Noordhoek JA, Broekema M, Kapus A. House Dust Mite-promoted Epithelial-to-mesenchymal Transition in Human Bronchial Epithelium. Am J Respir Cell Mol Biol 2009 Apr 16.

(12) Lordan JL, Bucchieri F, Richter A, Konstantinidis A, Holloway JW, Thornber M, et al. Cooperative effects of Th2 cytokines and allergen on normal and asthmatic bronchial epithelial cells. J Immunol 2002 Jul 1;169(1):407-14.

(13) Heijink IH, Vellenga E, Oostendorp J, de Monchy JG, Postma DS, Kauffman HF. Exposure to TARC alters beta2-adrenergic receptor signaling in human peripheral blood T lymphocytes. Am J Physiol Lung Cell Mol Physiol 2005 Jul;289(1):L53-L59.

(14) Slebos DJ, Ryter SW, van der TM, Liu F, Guo F, Baty CJ, et al. Mitochondrial localization and function of heme oxygenase-1 in cigarette smoke-induced cell death. Am J Respir Cell Mol Biol 2007 Apr;36(4):409-17.

(15) Woo PL, Cercek A, Desprez PY, Firestone GL. Involvement of the helix-loop-helix protein Id-1 in the glucocorticoid regulation of tight junctions in mammary epithelial cells. J Biol Chem 2000 Sep 15;275(37):28649-58.

(16) Tunggal JA, Helfrich I, Schmitz A, Schwarz H, Gunzel D, Fromm M, et al. E-cadherin is essential for in vivo epidermal barrier function by regulating tight junctions. EMBO J 2005 Mar 23;24(6):1146-56.

(17) Wetering van S, Zuyderduyn S, Ninaber DK, van Sterkenburg MA, Rabe KF, Hiemstra PS. Epithelial differentiation is a determinant in the production of eotaxin-2 and -3 by bronchial epithelial cells in response to IL-4 and IL-13. Mol Immunol 2007 Feb;44(5):803-11.

(18) Fukuda M, Nishida T, Otori T. Role of actin filaments and microtubules in the spreading of rabbit corneal epithelial cells on the fibronectin matrix. Cornea 1990 Jan;9(1):28-35.

(19) Keese CR, Wegener J, Walker SR, Giaever I. Electrical wound-healing assay for cells in vitro. Proc Natl Acad Sci U S A 2004 Feb 10;101(6):1554-9.

(20) Soong HK, Dass B, Lee B. Effects of cytochalasin D on actin and vinculin in cultured corneal epithelial cells. J Ocul Pharmacol 1990;6(2):113-21.

Figure legends

Figure 1. Attachment, growth and cell-cell contact formation characteristics of 16HBE14o- cells. 16HBE14o- cells were seeded in duplicates into ECIS arrays at different concentrations. **A)** Resistance and **B)** capacitance were monitored immediately after transfection in a time course of 96 hrs at 400 Hz and 40 kHz. To correct for the well-to-well variance, we normalized resistance and capacitance values to the starting point at the uncovered electrode. Initial well-to-well variance was not significantly different when cells were inoculated at different concentrations. Resistance values of the uncovered electrodes typically varied between 500-700 Ω and capacitance values varied between 60-80 nF. Results shown are representative of three independent experiments. **C)** $75*10^3$cells/well were grown on LabTeks for 24 and 72 hours and E-cadherin and ZO-1 were detected by immunofluorescent staining.

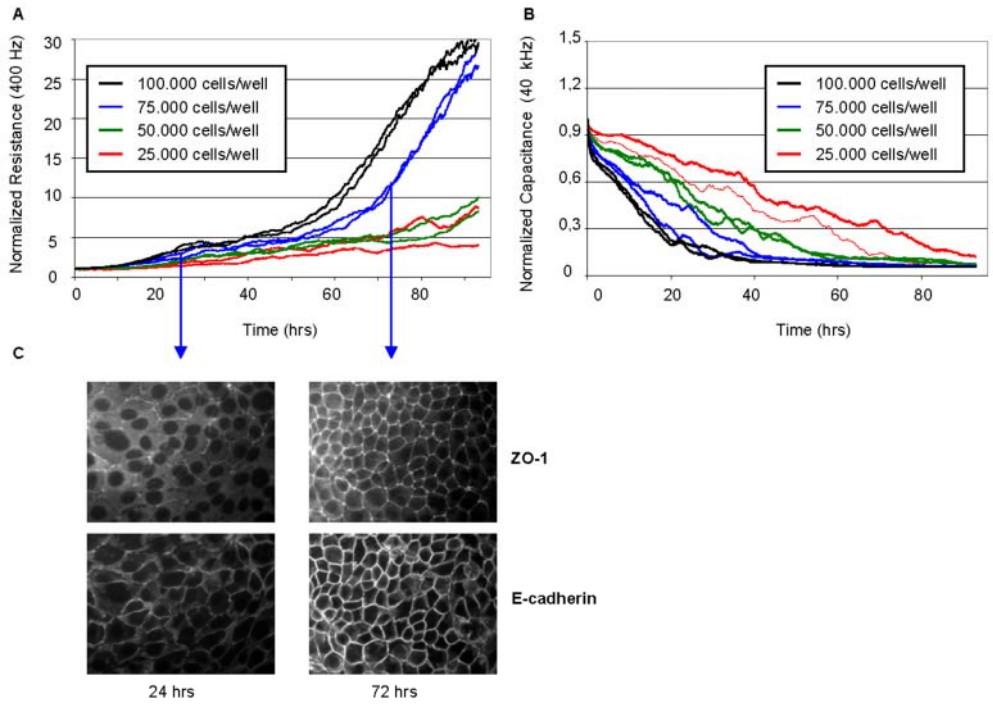

Figure 1

Figure 2. Reduced low-frequency-resistance upon disruption of intercellular contacts. 16HBE14o- cells were seeded at a density of 2.5-10*10^4/well into collagen-coated ECIS arrays and transfected with either the non-targeting control siRNA or specific E-cadherin siRNA oligonucleotides. On the following day, 16HBE14o- cells were

seeded in triplicates into ECIS arrays at different concentrations or 24 well plates. **A)** Resistance was measured in triplicates 0-60 hours after transfection by ECIS at 400 Hz. Mean normalized resistance (± SEM) is shown. **B)** Capacitance was measured in triplicates 0-60 hours after transfection by ECIS at 40 kHz. Mean normalized capacitance (± SEM) is shown. **C)** 16HBE14o- cells were seeded at a density of 2.5-10*10^4/well in triplicates into collagen-coated 24 well plates and transfected with either the non-targeting control siRNA or specific E-cadherin siRNA oligonucleotides Total cell lysates were prepared after 24 and 72 hours and E-cadherin was detected by western blotting. **D)** ZO-1 was detected by western blotting in total cell lysates of cells transfected with either the non-targeting control siRNA or specific E-cadherin siRNA oligonucleotides after 72 hours. **E)** Cells were seeded in duplicates into ECIS arrays. After 48 hours, when cells reached confluence, medium was replaced by serum-free medium. After 48 hours, Ca^{2+} was depleted. Normalized resistance at 400 Hz is shown. **F)** Cells were seeded in duplicates into ECIS arrays or LabTeks. After serum deprivation overnight, Ca^{2+} was depleted for 10 minutes. E-cadherin was detected by immunofluorescent staining.

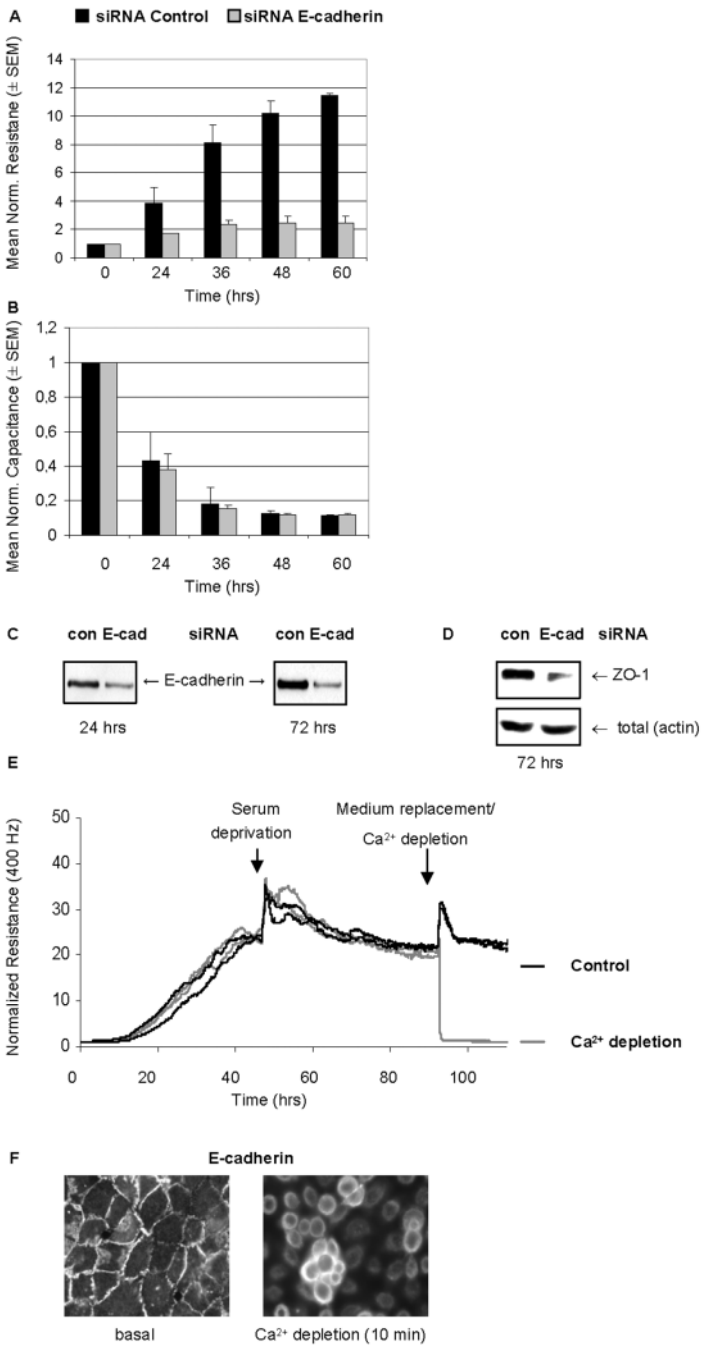

Figure 2

Figure 3. Attachment, growth and cell-cell contact formation characteristics of **A)** BEAS-2B cells **B)** A549 cells **C)** NCI-H292 cells **D)** PBEC derived from a healthy donor. Cells were seeded in duplicates onto collagen-coated ECIS arrays. Resistance and capacitance were measured immediately after seeding in a time course of 72 hrs

at 400 Hz and 40 kHz, resp., by ECIS. No differences were observed in the starting values of the different cell types upon inoculation (varying from 500-700 Ω and 60-80 nF, respectively) and to correct for the well-to-well variance, we normalized resistance and capacitance values to the starting point at the uncovered electrode. For PBEC, medium was replaced by hormone/growth factor-deprived medium (BEBM) after 48 hours. Results shown are representative of three independent experiments.

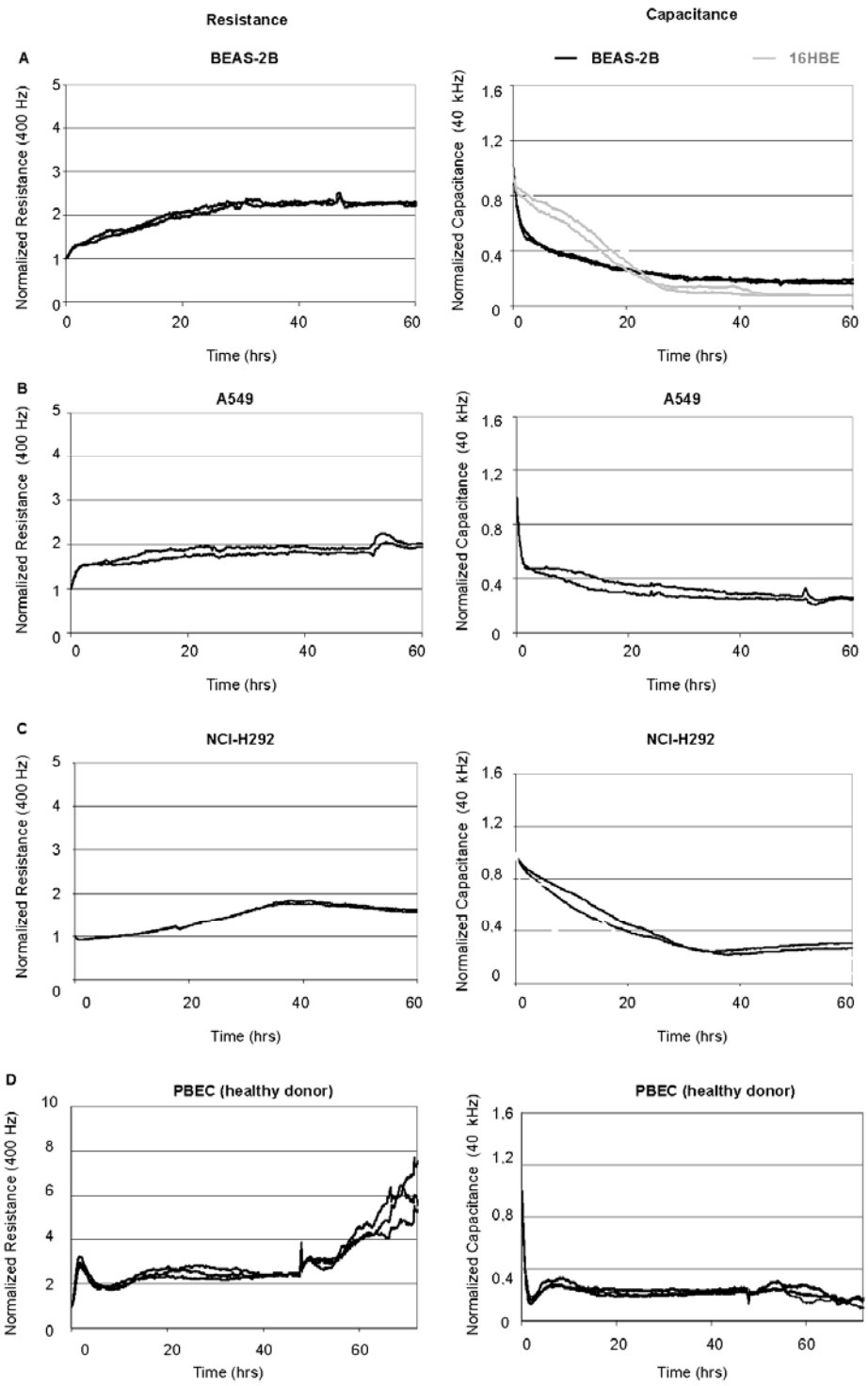

Figure 3

Figure 4. The ability to form epithelial junctions is related to the expression and localization of cell adhesion molecules. **A)** 16HBE14o-, NCI-H292, BEAS-2B and A549 cells or PBEC from asthma, COPD and healthy donors (*n=3*) were seeded in

duplicates in 24 well plates and cultured to confluence (48-72 hours). Cells were serum/growth factor-deprived overnight and total cell lysates were prepared. ZO-1 and E-cadherin were detected by western blotting (arrows). β-actin was used as a control for equal loading. **B)** PBEC from an asthma patient, a COPD patient and 3 healthy donors (I,II,III) were seeded in duplicates into ECIS arrays. Normalized resistance was measured immediately after seeding in a time course of 60 hrs at 400 Hz by ECIS. **C)** 16HBE14o-, NCI-H292, BEAS-2B, A549 and PBEC derived from healthy donors were seeded in duplicates in LabTeks and cultured to confluence (48-72 hours). ZO-1 and E-cadherin were detected by immunofluorescent staining. **D)** 16HBE14o-, NCI-H292, BEAS-2B, A549 cells and PBEC derived from healthy donors were seeded in duplicates in LabTeks and cultured to confluence (48-72 hours). F-actin was visualized by Rhodamine phalloidin staining. Representative results are shown.

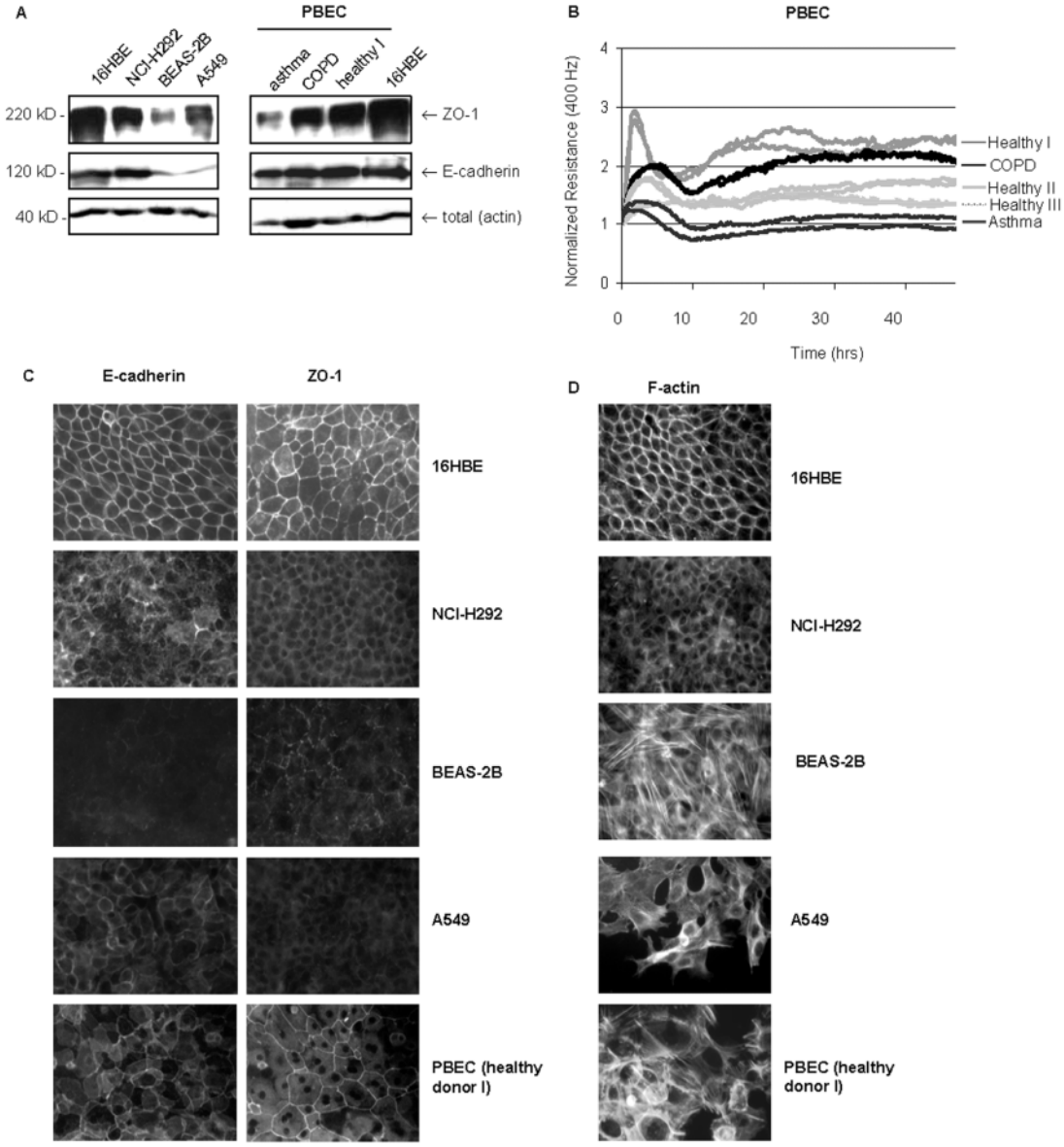

Figure 4

Figure 5. Differences in 16HBE14o- cells and BEAS-2B cells in migration response and recovery of epithelial barrier upon wounding by electroporation. **A)** 16HBE14o- cells were seeded in duplicates into ECIS arrays. After 48 hours, cells were serum-deprived overnight. A wound was applied by electroporation. Immediately and 1 ½

after wounding, arrays were taken out, cells were washed and pictures were taken. **B)** 16HBE14o- cells **C)** BEAS-2B cells were seeded in duplicates into ECIS arrays. After 48 hours, cells were serum-deprived overnight. A wound was applied by electroporation. Resistance and capacitance were measured in a time course of 3 hours prior to 15 hours after wounding at 400 Hz and 40 kHz, resp., by ECIS. Normalized values are shown.

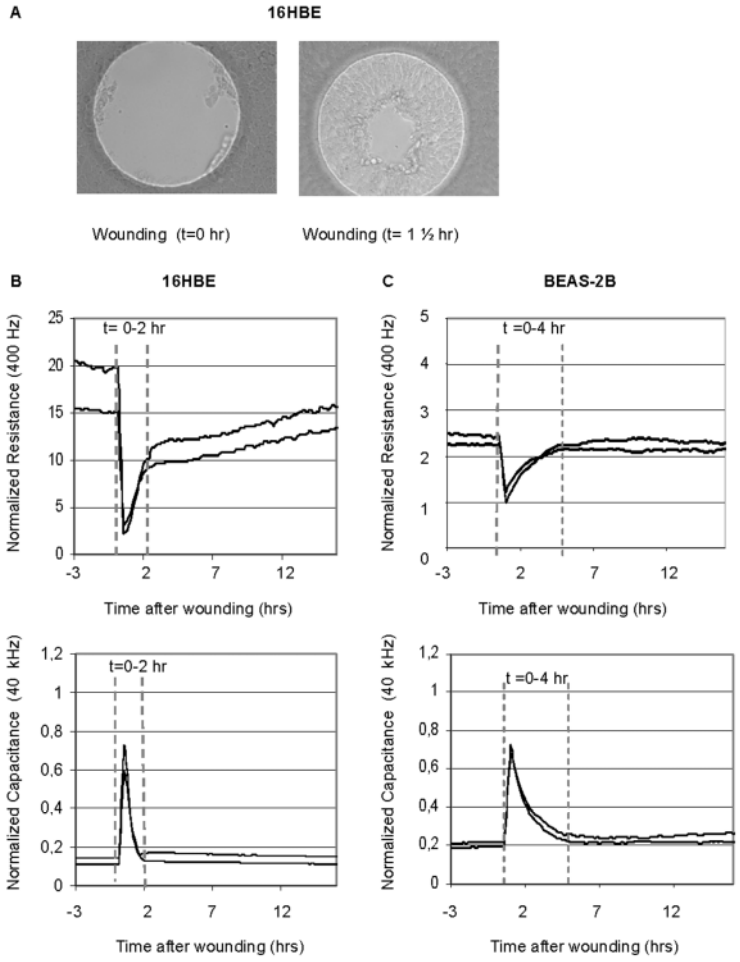

Figure 5

TABLE I. Adhesive characteristics of different airway epithelial cell types

Cell type / Features	16HBE14o-	BEAS-2B	NCI-H292	A549	PBEC

Resistance (400 Hz) at 72 hrs	12000-20000	1400-1600	1000-1200	1200-1500	2000-5000
Electrode coverage upon seeding ($75x10^3$ cells)	30-50 hrs	2,5-20 hrs	30-40 hrs	2,5-15 hrs	2-10 hrs
TJ protein ZO-1 at 72 hrs:					
- expression	high	low	moderate	low	moderate
- localization at junctions	yes	fragmented	no	no	yes
F-actin organization	cortical	stress fibers	cortical	stress fibers	stress fibers

TJ: tight junction.